

Cross-orientation masking in human color vision

José M. Medina

McGill Vision Research, Department of Ophthalmology,
McGill University, Montreal, Quebec, Canada



Kathy T. Mullen

McGill Vision Research, Department of Ophthalmology,
McGill University, Montreal, Quebec, Canada



Detection of a Gabor pattern is impaired in the presence of a similar pattern of orthogonal orientation, a phenomenon known as cross-orientation masking (XOM). Here we investigate the role of color in cross-orientation masking. We measured contrast detection thresholds to horizontally oriented Gabors overlaid by similar Gabors of a different orientation. Red-green chromatic masking was compared to achromatic masking for a wide range of spatial and temporal frequencies, orientations, and masks contrasts. We find that cross-orientation masking is significantly greater for chromatic than achromatic contrast. We also find it is invariant with the spatio-temporal conditions used, unlike achromatic cross-orientation masking that is known to have a spatio-temporal dependence (greatest for low spatial frequencies at high temporal frequencies). Furthermore, chromatic masking is isotropic (invariant across the orientation difference between test and mask), whereas the achromatic version of the masking effect displays orientation tuning, a phenomenon that was originally used to indicate the presence of orientationally selective mechanisms in human vision. We conclude that the P cell pathway or its projections can support cross-orientation masking. We propose distinct physiological origins for chromatic and achromatic masking, with a predominantly cortical site for chromatic masking in contrast to the M cell subcortical influences on achromatic masking suggested by previous studies.

Keywords: cross-orientation masking, orientation tuning, psychophysics, color vision, contrast-gain control

Citation: Medina, J. M., & Mullen, K. T. (2009). Cross-orientation masking in human color vision. *Journal of Vision*, 9(3):20, 1–16, <http://journalofvision.org/9/3/20/>, doi:10.1167/9.3.20.

Introduction

Orientation is a fundamental dimension in the perception of most visual scenes that has been studied extensively for almost half a century (Blakemore & Campbell, 1969; Campbell & Kulikowski, 1966; Hubel & Wiesel, 1959, 1963, 1968; Hubel, Wiesel, & Stryker, 1977; Phillips & Wilson, 1984). Psychophysical studies have used adaptation and visual masking techniques to investigate the presence of orientation-tuned mechanisms in vision, typically revealed by the systematic elevation in detection or discrimination threshold that occurs as the orientation difference between a test stimulus and a masking or adapting stimulus is reduced (Breitmeyer, 1984, 2007; De Valois & De Valois, 1988; Graham, 1989; Howard, 1982). In much of these data, however, some residual threshold elevation remains even for large orientation differences of up to 90 degrees between test and mask stimuli. This indicates the presence of interactions between stimuli that cannot be accounted for by traditional “within-channel” models of grating detection based solely on the responses of independent, orientation-tuned detection mechanisms (Baker & Meese, 2007; Campbell & Kulikowski, 1966; Meese & Hess, 2004; Phillips & Wilson, 1984; Snowden, 1992).

Cross-orientation masking (XOM), in which the detection of a test grating is masked by a superimposed

stimulus at an orthogonal orientation, is now widely accepted in human vision and indicates the presence of “cross-channel” interactions between test and mask that act to suppress the detection and visibility of the test stimulus (Baker & Meese, 2007; Cass & Alais, 2006; Chen & Foley, 2004; Foley, 1994; Holmes & Meese, 2004; Meese, Challinor, & Summers, 2008; Meese & Hess, 2004; Meese & Holmes, 2007; Meese, Summers, Holmes, & Wallis, 2007; Meier & Carandini, 2002; Petrov, Carandini, & McKee, 2005; Ross & Speed, 1991; Ross, Speed, & Morgan, 1993; Vimal, 1998). It is thought that the psychophysical phenomenon of XOM is linked to the physiological effect of cross-orientation suppression (XOS) observed in single neurons in the mammalian visual cortex. In XOS, a masking stimulus, which does not activate the test neuron when presented alone, produces suppressive effects on a neuron’s response to a test stimulus that occurs even when the test and mask stimuli are at orthogonal orientations (Bonds, 1989; Carandini, Heeger, & Movshon, 1997; DeAngelis, Robson, Ohzawa, & Freeman, 1992; Heeger, 1992; Li, Peterson, Thompson, Duong, & Freeman, 2005; Morrone, Burr, & Maffei, 1982; Sengpiel & Vorobyov, 2005; Walker, Ohzawa, & Freeman, 1998). The physiological origins of XOS are thought to be cortical although there is also evidence in the cat suggesting the involvement of a subcortical and monocular site (Carandini, Heeger, & Senn, 2002; Freeman, Durand, Kiper, & Carandini, 2002; Li et al.,

2005; Priebe & Ferster, 2006; Sengpiel & Vorobyov, 2005; Truchard, Ohzawa, & Freeman, 2000; Walker et al., 1998). The modification of the contrast response function of cortical neurons by contrast normalization is part of a process of contrast gain control that serves to increase the contrast range over which cortical neurons can effectively respond and maintain stimulus selectivity (Carandini & Heeger, 1994; Geisler & Albrecht, 1992; Heeger, 1992; Levitt & Lund, 1997; Peirce, 2007; Tolhurst & Heeger, 1997). In a more general sense, however, the psychophysical phenomenon of cross-orientation masking indicates the presence of nonlinearities in the visual system tuned to different orientations and spatial frequencies.

Two different forms of orientation masking have been explored. One is surround masking, in which the masker is placed remotely from the test, and the other, the main focus of this study, is overlay masking, in which both masker and test are spatially co-extensive. Surround masking is a different type of masking since it displays greater tuning for orientation and spatial frequency and occurs more strongly in the periphery than the fovea (Meese, Summers, et al., 2007; Petrov et al., 2005; Snowden & Hammett, 1998; Solomon, Sperling, & Chubb, 1993; Xing & Heeger, 2000; Yu & Levi, 2000). As it occurs for masks placed remotely from the test stimulus, it is more indicative of long-range cortical interactions and the operation of extra striate feedback. Overlay masking, on the other hand, is broadly tuned to orientation and spatial frequency and is found in central vision.

Although at first thought to be a general effect occurring across a range of test spatial and temporal frequencies, XOM has more recently been shown to be greatest for test stimuli at low spatial (0.5 cpd) and mid-high temporal frequencies (4–15 Hz), with the least effect occurring at high spatial (8 cpd) and low temporal frequencies (0.5 Hz) (Cass & Alais, 2006; Meese & Holmes, 2007). This spatio-temporal signature potentially suggests an association of XOM with the M cell pathway, which has its greatest sensitivity in this spatio-temporal range (Merigan & Maunsell, 1993). Such a potential association allows us to make direct predictions concerning the involvement of color in cross-orientation masking, which we explore in this paper. Since P cells, and not M cells, respond robustly to red-green color contrast, a selective involvement of M cells in XOM would suggest XOM is weak or absent for color vision.

Here we investigate whether color can support cross-orientation masking in red-green color vision, using red-green isoluminant stimuli and achromatic stimuli for comparison with the luminance system. So far, XOM in color vision has not been directly explored and yet interest in the role of color vision in orientation processing has been very strong for two reasons. First, orientation tuning is an indicator for the role that color contrast plays in spatial vision as it is a fundamental requirement for form processing. Second, the neurophysiological basis of orientation in color vision in the cortex is complex and

unresolved with distinct populations of neurons; one population is orientation tuned for color contrast but relatively unselective for color in that it also responds to luminance contrast, and another smaller population with a highly selective color sensitivity but lacking orientation tuning (Johnson, Hawken, & Shapley, 2008; Solomon & Lennie, 2005). The functional significance of these different groups of neurons for color vision is a challenging and unresolved issue. In this paper, we investigate the role that orientation plays in contrast-gain control in color vision as a significant step in unraveling the role of orientation processing in color vision. We address three issues: the extent that XOM is found in color vision, its dependence across spatial and temporal frequency, and its orientation tuning.

Methods

Apparatus

Stimuli were displayed on a CRT color monitor (Mitsubishi Diamond Pro 2070SB, resolution of 1024 × 768 and a frame rate of 120 Hz) connected to a graphics card (Cambridge Research Systems, VSG 2/5) in a generic PC. This graphics card has over 14 bits of contrast resolution and is specialized for the measurement of visual thresholds. The gamma nonlinearity of the luminance output of the monitor guns was corrected in look-up tables using a Cambridge Research Systems OptiCal photometer. The spectral outputs of the red, green, and blue phosphors of the monitor were calibrated using a PhotoResearch PR-645 SpectraScan spectroradiometer. The CIE-1931 chromaticity coordinates of the red, green, and blue phosphors were ($x = 0.631$, $y = 0.340$), ($x = 0.299$, $y = 0.611$), and ($x = 0.147$, $y = 0.073$), respectively. The background was achromatic with a mean luminance of 46.1 cd/m² at the screen center.

Observers

The observers were the two authors (J.M. and K.T.M). Both had normal vision and normal color vision according with the Farnsworth-Munsell 100-Hue test and both had experience in contrast threshold experiments. Observers were seated 60 cm from the monitor in a dimly lit room and wore corrective lenses if required. The experiments were performed in accordance with the Declaration of Helsinki.

Color space and stimuli

Stimuli were represented in a three-dimensional cone-contrast space (Cole, Hine, & McIlhagga, 1993; Eskew, McLellan, & Giulianini, 1999; Sankeralli & Mullen,

1996) in which each axis is defined by the incremental stimulus intensity for each cone type to a given stimulus normalized by the respective intensity of the fixed adapting white background. Cone excitations for the L-, M-, and S-cones were calculated using the cone fundamentals of Smith and Pokorny (1975). A linear transform was calculated to specify the required phosphor contrasts of the monitor for given cone contrasts. Postreceptoral luminance and red-green cone-opponent mechanisms were modeled as linear combination of cone contrast responses. They were isolated in the achromatic ($L + M + S$) and red-green ($L - \alpha M$) cardinal axis, where α is a numerical constant obtained at isoluminance. Stimulus contrast is defined as the root mean square or the vector length in cone contrast units (C_C):

$$C_C = \sqrt{(L_C)^2 + (M_C)^2 + (S_C)^2}, \quad (1)$$

where L_C , M_C , and S_C , represent the L, M, and S Weber cone-contrast fractions in relation to the L, M, and S cone values of the achromatic background. This metric differs by a factor of $\sqrt{3}$ from the conventional luminance contrast. Both chromatic and achromatic test stimuli were horizontally oriented Gabor patterns. Three different

spatial frequencies were tested (phase = 0): 0.375, 0.75, and 1.5 cpd (see stimulus pictures in Figures 1A and 1B). At the viewing distance of 60 cm, all the Gaussian envelopes of the Gabor stimuli were scaled to a fixed space constant of $\sigma = 2^\circ$; σ expressed in terms of the number of spatial stimulus cycles is 0.75, 1.5, and 3 cycles at 0.375, 0.75, and 1.5 cpd, respectively. Gabors were sinusoidally phase reversed in time at three different temporal frequencies: 2, 4, and 8 Hz. All the Gabors were presented in a contrast modulated temporal Gaussian envelope ($\sigma = 0.125$ s; interval duration, 1 s, see Figure 1C).

In the XOM experiments, the mask stimuli were spatially orthogonal, i.e., they were vertically oriented Gabor patterns. In the orientation tuning experiments, mask orientation varied clockwise from the horizontal in steps sizes of 15° , 30° , 45° , 60° , and 90° (orientation of test stimulus was fixed at the reference horizontal position). In both XOM and orientation tuning experiments, the mask stimulus has the same spatio-temporal frequency, phase, and color properties as the test stimulus. Both test and mask stimuli were controlled independently by lookup tables and were interlaced with frame-by-frame cycling. The mask contrast modulation was limited by the color gamut of the monitor and the monitor frame interleaving. The maximum available for chromatic

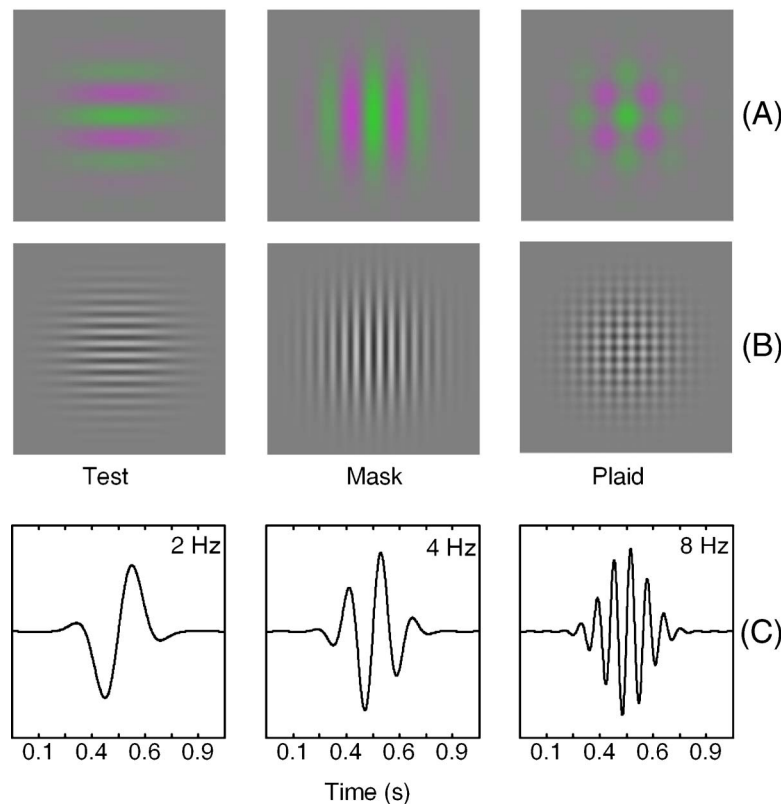


Figure 1. Representation of the test and masker Gabor stimuli and the two stimuli superimposed (i.e., a plaid) at high contrasts under different spatio-temporal configurations. All the Gabor stimuli used in the experiments had a fixed space constant of $\sigma = 2^\circ$. (A) An example of a red-green isoluminant Gabor (0.375 cpd) and (B) an achromatic Gabor (1.5 cpd). (C) Sinusoidal temporal waveforms in a Gaussian envelope at 2, 4, and 8 Hz.

gratings was 2.1% ($3.6/\sqrt{3}$), and for achromatic gratings, 28.9% ($50/\sqrt{3}$).

For each observer and for each spatial and temporal frequency, the isolation of the red-green mechanism at isoluminance (value of α above) was estimated by a minimum motion task in the cone contrast space (Cavanagh, Tyler, & Favreau, 1984). Gabor settings were defined at the two orientations corresponding to the test and mask stimulus, separately. In both cases, the minimum motion perceived of the Gabor grating was established using a method of adjustment. A small black fixation point was displayed during the minimum motion task. In each orientation, a minimum of 10 settings were measured. Isoluminance was calculated as the arithmetic mean of both conditions together of at least 20 settings. Luminance artifacts in chromatic gratings were minimized according with the range of low spatial frequencies selected ($0.375\text{--}1.5$ cpd, $\sigma = 2^\circ$) (Bradley, Zang, & Thibos, 1992).

Procedure

We measure binocular contrast detection thresholds in fovea using natural pupils. We first measured contrast detection thresholds in both the horizontal and vertical orientations in the absence of a mask. A two-alternative forced-choice staircase procedure was used with presentation intervals (1 s each), separated by 0.5 s. The subject indicated in which interval the stimulus appeared (the other was blank). Next, we measured contrast detection thresholds in the presence of a mask stimulus using a similar staircase procedure. In both time intervals, a vertically oriented mask stimulus was presented at a specific cone contrast value. In one of the two intervals, a horizontally oriented test stimulus with the same spatio-temporal and color configuration was superimposed with a lower contrast (i.e., a plaid, see Figures 1A and 1B). The subject indicated which interval contained the test stimulus.

A “2-down, 1-up” weighted staircase was used with audio feedback. A reversal was defined when the subject responded incorrectly after a minimum of two consecutive correct responses. Each staircase terminated after six reversals. The first reversal was used to establish the threshold level. After first reversal, stimulus contrast was raised by 25% following one incorrect response and lowered by 12.5% following two consecutive correct responses. For a given staircase session, the number of total trials fluctuated between 30 and 60 trials. The threshold value was calculated as the arithmetic mean of the last five reversals of the staircase at the 81.6% correct detection level. Each plotted threshold is based on the arithmetic mean of a minimum of four staircase measurements. A small black fixation point was displayed during interstimulus intervals. Data were collected for both red-green and achromatic stimuli.

Results

The effect of mask contrast

The effect of the orthogonal mask on test detection thresholds is shown as a function of mask contrast (TvC functions) in Figures 2 and 3 for two subjects, J.M. and K. T.M., respectively.

The form of the achromatic TvC functions demonstrates nonlinear effects (a U-shaped function) and is in agreement with previous studies (Baker & Meese, 2007; Cass & Alais, 2006; Chen & Foley, 2004; Foley, 1994; Holmes & Meese, 2004; Meese & Holmes, 2007; Meese, Holmes, & Challinor, 2007; Meese, Summers, et al., 2007; Meier & Carandini, 2002; Petrov et al., 2005; Vimal, 1998). For all achromatic conditions and for each observer, the mask produces a significant elevation of the test contrast threshold (XOM) (all conditions, Kruskal–Wallis test, $P < 0.05$) occurring over a wide range of mask contrasts from 10 to 120 multiples of detection threshold. For both observers, XOM for achromatic stimuli has a spatio-temporal dependence, in which the masking decreases as the temporal frequency decreases and spatial frequency increases (Cass & Alais, 2006; Meese & Holmes, 2007; Meese, Summers, et al., 2007; Phillips & Wilson, 1984). This is shown in our data by a fit of the slopes of the TvC functions in the masking region by a linear regression (least squares fit in linear coordinates). The slope values are indicated in Figures 2 and 3.

The XOM masking functions for isoluminant red-green stimuli clearly differ from the achromatic ones; chromatic masking is greater and rises more steeply than the equivalent achromatic masking, as shown by the higher values of the fitted slopes for the chromatic data. (We note that at the highest temporal frequency of 8 Hz, the high detection thresholds limit the range of mask contrasts that could be used to 5–6 times detection threshold, which is an insufficient range to obtain masking functions.) There is little evidence for any variation in the fitted slopes for the chromatic masking with the spatio-temporal conditions used.

For the purposes of comparison, in Figure 4 we plot slope values as a function of each spatio-temporal condition expressed in terms of stimulus speed (TF/SF). A broadly similar comparison was made by Meese and Holmes (2007, their Figure 6) for achromatic stimuli, but with the strength of the masking determined from a model fit rather than by linear regression. Our achromatic data generally support the speed dependence reported by Meese and Holmes, although with poorer correlation coefficients, with the greatest XOM occurring at low spatial and high temporal frequencies. The chromatic data show a lack of speed dependence, with poor correlation coefficients. Figure 4 also shows that the chromatic

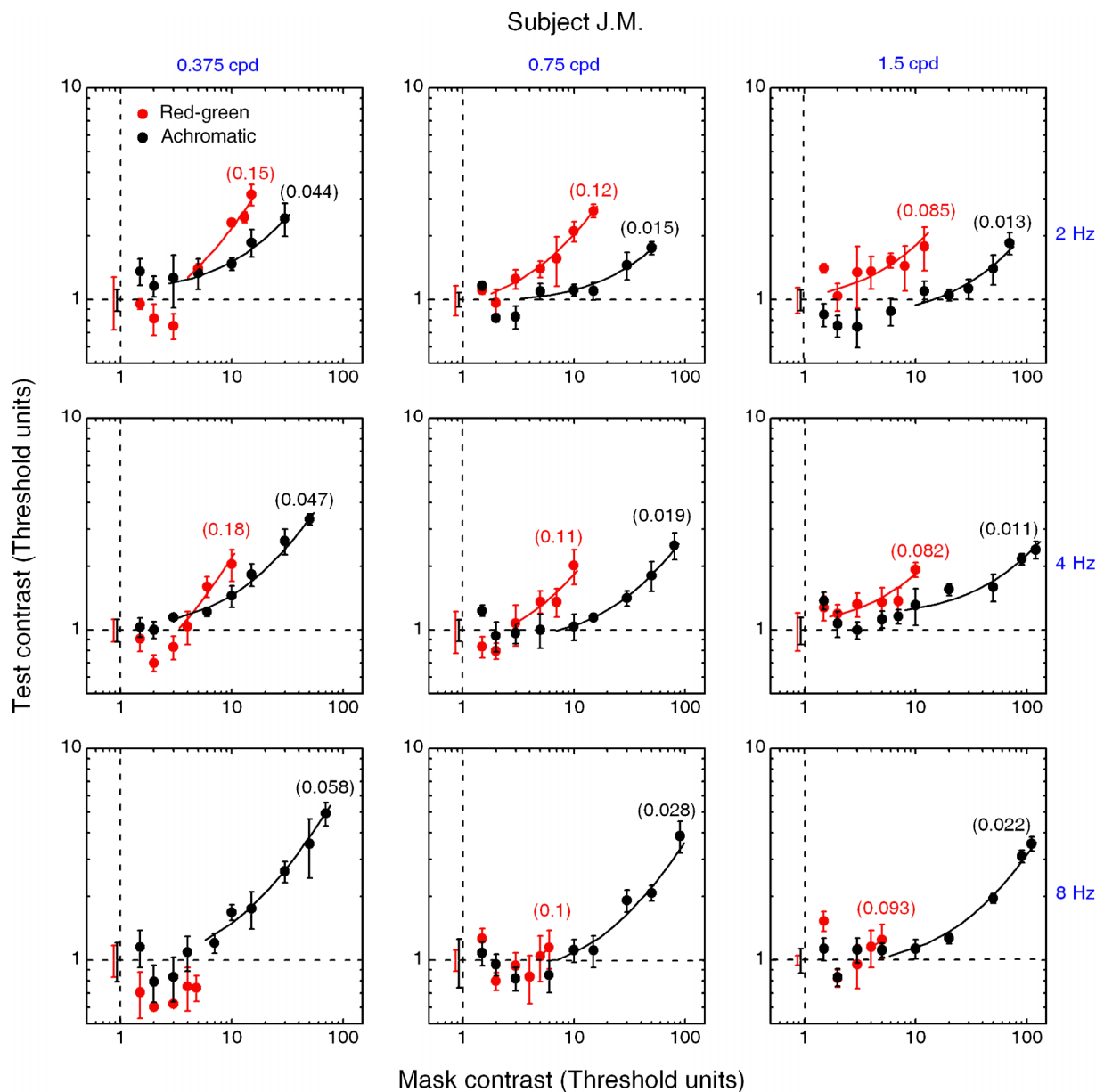


Figure 2. TvC functions for cross-orientation masking in color and achromatic vision. Test thresholds are plotted as a function of mask contrast in double logarithmic coordinates with each axis scaled in multiples of detection threshold. (If there was a significant difference between horizontal and vertical stimulus detection thresholds, the normalization values for both vertical and horizontal axis were used separately, otherwise an average was used.) Data are plotted for nine spatio-temporal configurations (0.375, 0.75, and 1.5 cpd, with 2, 4, and 8 Hz). Red and black solid symbols indicate test thresholds for red-green isoluminant and achromatic gratings, respectively. Red and black values in brackets indicate the estimated slopes by linear regression (red and black lines) for red-green isoluminant and achromatic gratings, respectively. Horizontal dotted lines indicate no effect of the mask on the test. Error bars are ± 1 standard deviation of the mean (observer J.M.).

masking slopes are steeper than the achromatic, a point which we analyze statistically in Figure 6.

To compare the masking functions in more detail, we have plotted the data for all nine spatio-temporal conditions using common axes in Figure 5, with color and observers shown separately. The chromatic cross-orientation masking (test contrast thresholds >1) shows little dependency on the spatio-temporal configuration,

i.e., the data almost collapse into a single scale. Maximum masking values are 3.1 and 1.9 multiples of detection threshold for J.M and K.T.M., respectively. At high masking contrasts, XOM becomes similar to Weber’s law with an average slope close to 0.1. For the achromatic stimuli, XOM spans a wider range than the chromatic (4.9 and 6.7 for J.M. and K.T.M., respectively), but this is only because a greater mask contrast range could be used for the

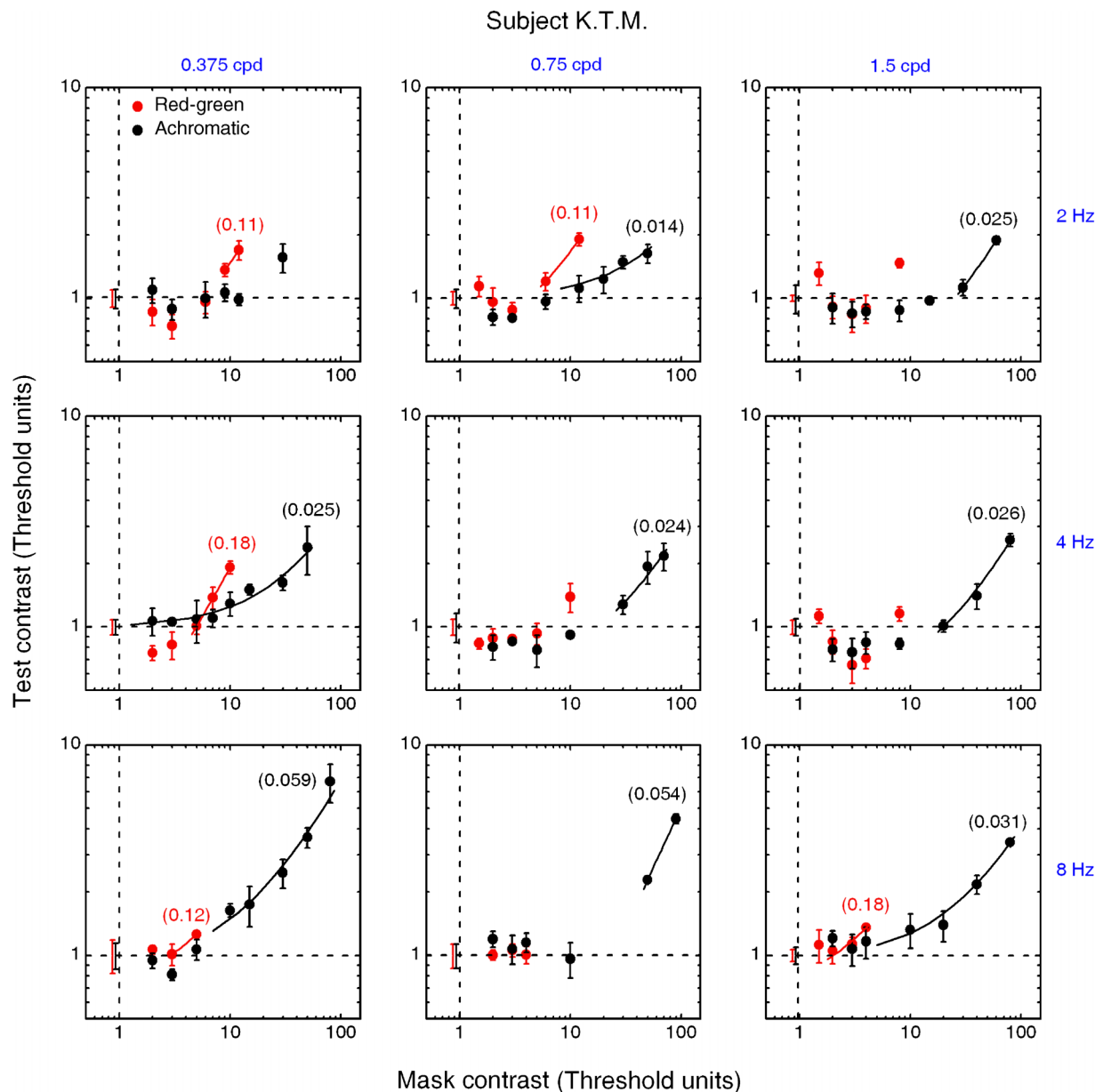


Figure 3. TvC functions for cross-orientation masking in color and achromatic vision. Details are as for Figure 2. Error bars are ± 1 standard deviation of the mean (observer K.T.M.).

achromatic stimuli. Figures 4 and 5 demonstrate that over the equivalent contrast range and at the higher mask contrasts, XOM is weaker for achromatic than chromatic conditions.

For most TvC functions in Figures 2 and 3, facilitation is apparent in the presence of a mask between 2 and 3 multiples of detection threshold, as reported before for achromatic stimuli (Meese & Holmes, 2007; Meese, Holmes, et al., 2007; Meese, Summers, et al., 2007; Petrov et al., 2005). This dipper effect at the lowest values was significant in both chromatic and achromatic conditions (two-sample independent *t*-test; all cases, $P < 0.05$) and

was slightly greater for chromatic stimuli than for achromatic stimuli. We note that these optimum thresholds are very low, demonstrating the strong suprathreshold facilitatory effect of the mask, which reduces threshold by up to 26–40%. Models of contrast masking have not yet conclusively explained this phenomenon (Chen & Foley, 2004; Henning & Wichmann, 2007; Meese & Holmes, 2007; Meese, Holmes, et al., 2007; Meese, Summers, et al., 2007; Pelli, 1985; Petrov et al., 2005; Vimal, 2002).

For each spatio-temporal configuration and for each observer, we compared the XOM obtained for both chromatic and achromatic stimuli at equivalent multiples

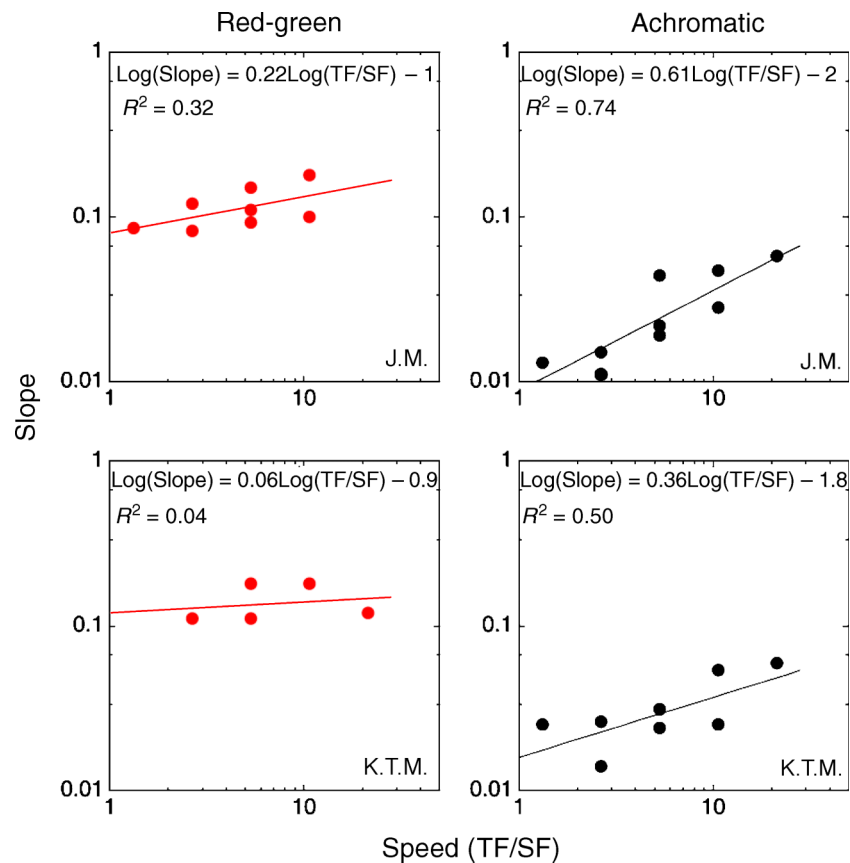


Figure 4. The slopes of the masking functions, as fitted in Figures 2 and 3, are plotted as a function of stimulus speed (TF/SF) on log–log axes. These data are fitted to a straight line using a least-squares method and the correlation coefficients (R^2) are given.

of the detection threshold using the following normalized masking ratio:

$$\frac{(C_{RG}/C_{RG_0})}{(C_{AC}/C_{AC_0})}, \quad (2)$$

where C_{RG} and C_{AC} represent the contrast detection threshold in the masking condition for the red-green isoluminant and achromatic stimuli, respectively. In both cases, the subscript “0” denotes the reference detection threshold. A masking ratio higher than unity indicates more masking for chromatic than achromatic stimuli and vice versa. Figure 6 represents, for each observer, the mean masking ratio averaged over all spatio-temporal conditions.

There was more masking for color at equivalent multiples of the threshold, for the observers J.M. (1.43) and K.T.M. (1.29). A t -test revealed significant differences from unity for J.M. and K.T.M. ($t = 5.29$, $P < 0.001$; $t = 3.46$, $P = 0.007$, respectively). Our results clearly indicate that TvC functions differ for chromatic and achromatic stimuli, with chromatic XOM significantly greater than achromatic over the testable range (2–4 Hz).

The effect of mask orientation

We explored the effect of the orientation of the mask on the test threshold by varying mask orientation relative to the test from 15 to 90 degrees. Figure 7A represents a semi-logarithmic plot of test contrast threshold (scaled in multiples of detection threshold), as a function of the relative test and mask orientations (TvO functions). In order to compare between chromatic and achromatic masking, we selected mask contrasts that provided the same level of cross-orientation masking in both cases, based on the TvC functions in Figures 2 and 3. Since color contrast is a more effective mask than achromatic contrast under cross-orientation conditions (90 degree mask), the color masks generally had a lower contrast (in multiples of detection threshold) than the achromatic masks. For example, in the top panels of Figure 7A, we used color masks with a contrast of 10 or 12 times detection threshold (for J.M. and K.T.M., respectively), but achromatic masks at 30 times detection threshold since these mask chromatic and achromatic contrasts are equal in their masking effect (i.e., no significant difference between chromatic and achromatic masking for relative orientations of 90 degrees; > 0.05 , Mann–Whitney test). The four panels of Figure 7A

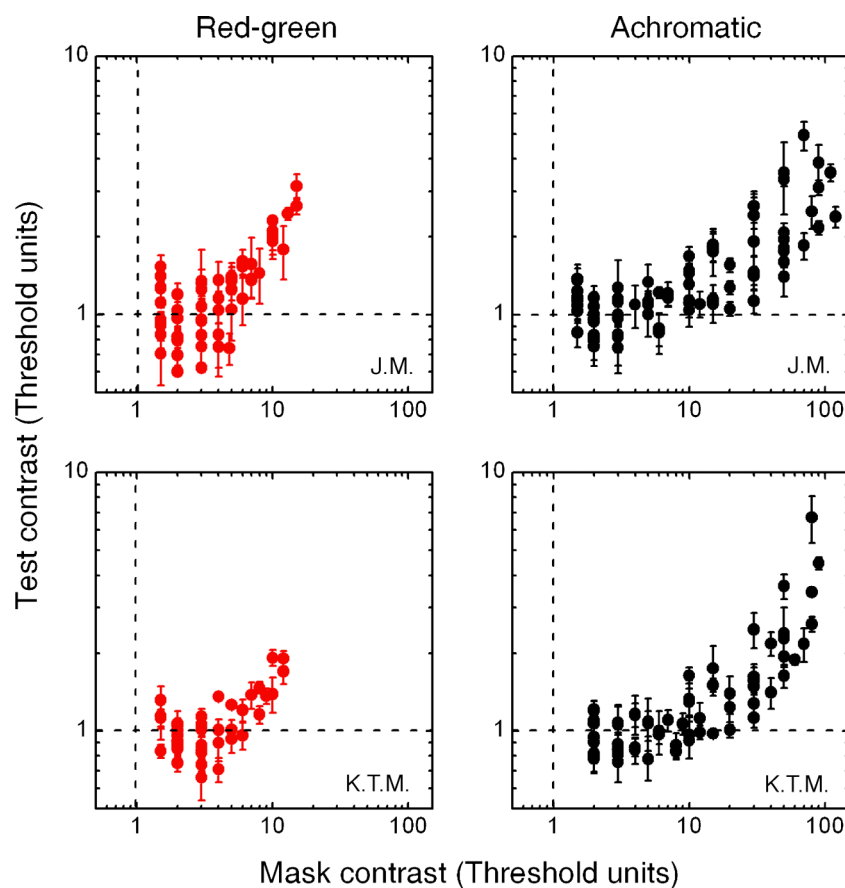


Figure 5. The data from all the spatio-temporal configurations are plotted together. Each axis is scaled in multiples of detection threshold contrasts. Red and black solid circles indicate test thresholds for red-green isoluminance and achromatic gratings, respectively. Horizontal dotted lines indicate no effect of the mask on the test so that points above and below unity indicate masking and facilitation, respectively. Vertical dotted lines indicate the limit determined by the detection threshold contrasts of the masker alone. Data are plotted separately for two observers (J.M. and K.T.M.). Error bars show ± 1 standard deviation.

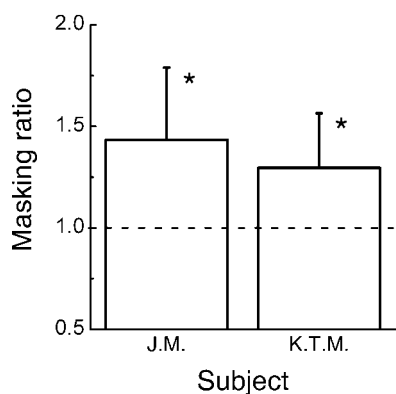


Figure 6. Normalized red-green over achromatic masking ratio averaged over all the spatial and temporal frequencies. Data are plotted separately for two observers (J.M. and K.T.M.). Error bars show ± 1 standard deviation. The asterisk highlights the existence of significant differences from unity in accordance with the *t*-test.

show results for two spatio-temporal conditions for each subject. Figure 7B represents the same data but grouped into achromatic and chromatic plots and normalized to the maximum cone contrast value so that the peaks coincide. This allows a better visual comparison between the different orientation tuning curves at different spatio-temporal frequencies and contrasts.

The chromatic TvO curves are almost flat suggesting extremely broad or absent orientation tuning (Vimal, 1997, 1998). Under some conditions in Figure 7A, there is even a reduction in the test contrast at the smallest orientation angle of 15° (K.T.M., 2 Hz–0.375 cpd). This is contrary to what is expected for an orientation-tuning curve, in which test threshold typically increases as the orientation difference decreases. The lack of any dependency on orientation for color vision was confirmed by an analysis of cone contrast thresholds at different angles (all cases, $P > 0.05$, Kruskal–Wallis). Therefore, the chromatic TvO functions are invariant, showing no dependency on either the orientation of the mask or the spatio-temporal configuration of the test (Figure 7B, left panel).

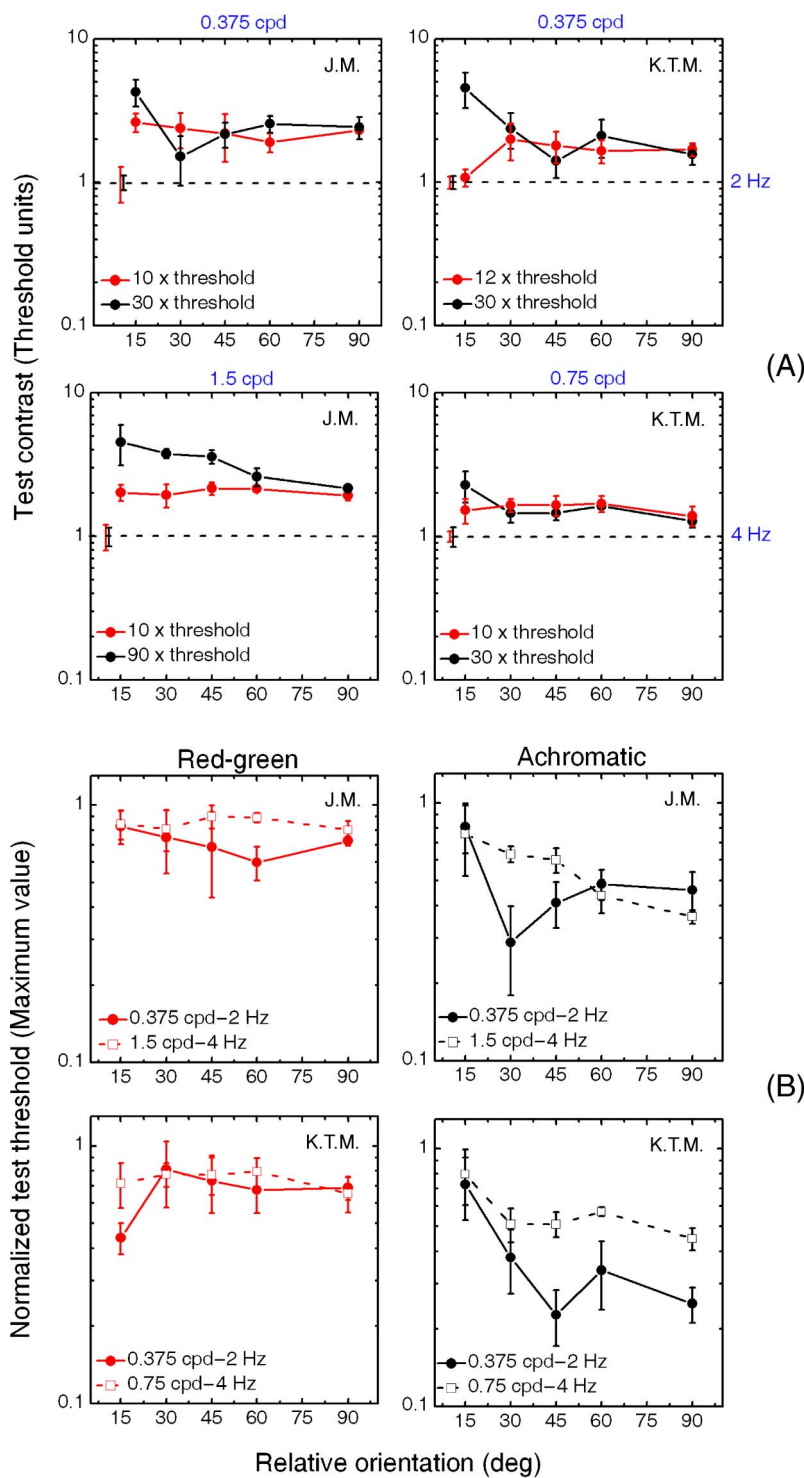


Figure 7. Effect of mask orientation on test threshold elevation (TvO). (A) The threshold elevation of the test stimulus (scaled in multiples of detection threshold) is plotted as a function of the orientation of the mask. Red and black symbols are for red-green isoluminant and achromatic gratings, respectively. Spatio-temporal conditions are as marked and plotted for two observers (J.M. and K.T.M.). Horizontal dotted lines indicate no effect of the mask on the test. Mask contrasts were selected to provide the same levels of cross-orientation masking for the chromatic and achromatic stimuli at 90 degrees and so these data points coincide. (B) The mask orientation data has been re-plotted to group the chromatic and achromatic data onto separate graphs so that the effect of the spatio-temporal conditions can be compared. Data have been normalized to the maximum cone contrast value to a peak height close to unity. *Left panels:* chromatic mask orientation. *Right panels:* achromatic mask orientation curves. In both cases, solid circles plus solid lines and open squares plus dashed lines indicate different spatio-temporal conditions. Error bars ± 1 standard deviation. We assumed orientation tuning is symmetrical so that only orientation angles between 0° and 90° are measured (Baker & Meese, 2007; Phillips & Wilson, 1984; Vimal, 1997).

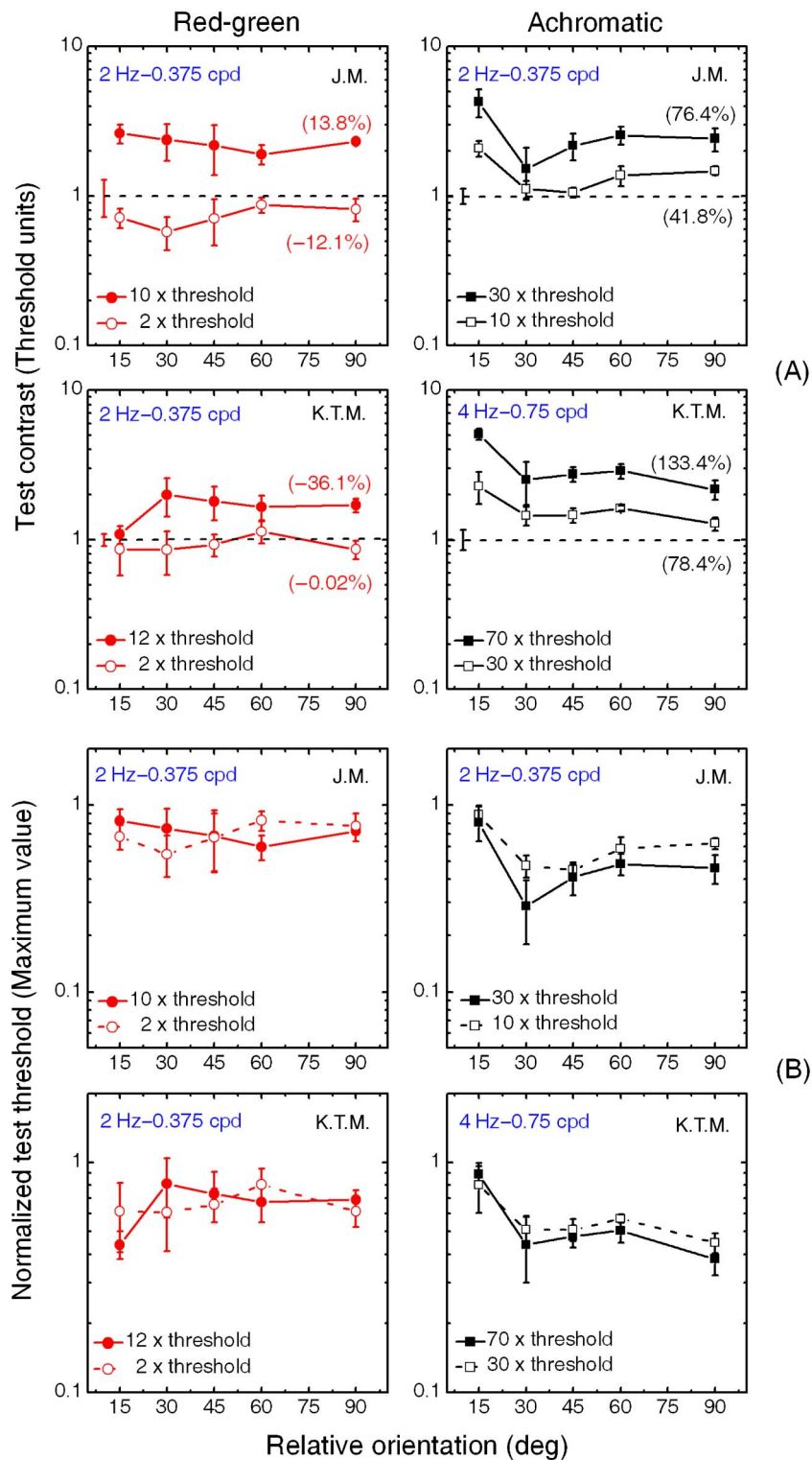


Figure 8. Contrast invariance of mask orientation curves in color vision. (A) Semi-logarithmic plot of the TvO functions at different mask contrast levels. Examples from each spatio-temporal configuration are plotted separately. The vertical axis is scaled in threshold units. Red circles and black squares connected by solid lines indicate test thresholds for red-green isoluminance and achromatic gratings, respectively. Horizontal dotted lines indicate no effect of the mask on the test so that points above and below 1 indicate masking and facilitation, respectively. For each tuning curve, the orientation modulation index is indicated in red and black between brackets at the right for red-green isoluminant and achromatic gratings, respectively. Data are plotted separately for two observers (J.M. and K.T.M.). (B) The same data normalized to a peak height of 1 to facilitate comparison. Symbols connected by solid and dashed lines indicate orientation-tuning curves inferred at different contrast levels. Error bars ± 1 standard deviation.

In contrast, the achromatic TvO curves depend on the relative orientation with a threshold elevation occurring at low mask orientation angles (Figure 7A), replicating the form of the dependence on mask orientation found previously for achromatic stimuli and used to establish the presence of orientation-tuned mechanisms for achromatic contrast (Baker & Meese, 2007; Bradley, Switkes, & De Valois, 1988; Campbell & Kulikowski, 1966; Phillips & Wilson, 1984; Snowden, 1992; Webster, De Valois, & Switkes, 1990). We confirmed the significance of this effect using an analysis on cone contrast thresholds at each spatio-temporal configuration ($P < 0.025$, Kruskal–Wallis). Achromatic TvO functions are also spatio-temporally dependent (Phillips & Wilson, 1984; Snowden, 1992). For example, for a fixed mask contrast, changing the spatial and temporal frequency can induce a variation in the test contrast relative to the maximum value at mask orientation angles higher than 15° (Figure 7B, right panel K.T.M.).

The effect of contrast on mask orientation curves

We examined the dependency of the TvO functions on mask contrast by selecting a range of mask contrasts from the TvC curves. Figure 8A represents several examples in a semi-logarithmic plot. Whereas in the previous plot we matched masks in terms of their masking effect (i.e., for equivalent elevations of test threshold), here we select low and high mask contrast for each condition. TvO curves are re-plotted for J.M. at 0.375 cpd–2 Hz (for RG at 10 times, and achromatic at 30 times detection threshold) and compared with new TvO curves obtained at the same spatial and temporal frequencies but lower mask contrasts (RG at 2 times, and achromatic at 10 times detection threshold). For K.T.M., TvO curves are re-plotted at 0.375 cpd–2 Hz for RG (12 times detection threshold) and for achromatic at 0.75 cpd–4 Hz (30 times detection threshold) and are compared with new TvO functions obtained at a lower RG mask contrast (2 times detection threshold) and a higher achromatic mask contrasts (70 times detection threshold) in order to span a wide contrast range. Figure 8B indicates the same data but normalized to peak amplitude of 1 for better visual comparison.

To quantify the amplitude of the orientation tuning inferred by masking, a modulation depth index (MD) was computed as the relative difference between the contrast thresholds for masks at 15° and 90° (in %), following a previous definition by Sharon and Grinvald (2002), is displayed in Figure 8A.

$$\text{MD} = \left(\frac{C_{15^\circ} - C_{90^\circ}}{C_{90^\circ}} \right) \times 100. \quad (3)$$

A value of 0 represents no modulation whereas positive and negative values indicate a threshold elevation or

reduction at 15° , respectively. Chromatic TvO functions at low mask contrasts were again flat, showing no dependency on the orientation angle (all cases, $P > 0.05$, Kruskal–Wallis on cone contrast thresholds). The degree of orientation selectivity is low and in some cases inverted as indicated by the negative orientation modulation values. The corresponding chromatic TvO curves at higher and lower mask contrasts overlap (Figure 8B, left panels), indicating contrast invariance.

Achromatic TvO functions were orientation dependent but the effect is somewhat weaker at low mask contrast (all cases, $P < 0.05$, Kruskal–Wallis on cone contrast thresholds). Achromatic TvO curves have sharper orientation tuning (Figure 8A, right panels) with a stronger threshold elevation at 15° at higher mask contrasts as indicated by the orientation modulation values (from 42% to 133%). However, achromatic orientation tuning curves are also minimally affected by the mask contrast level selected and almost overlap (Figure 8B, right panels). This condition qualitatively agrees with a contrast invariance of orientation tuning.

Discussion

We have demonstrated that cross-orientation masking occurs in color vision but has significant differences from the equivalent masking in achromatic vision. Specifically, chromatic XOM is significantly greater for human color vision than for achromatic vision over the whole range of spatial and temporal frequencies for which chromatic masking can be measured. We also show that chromatic XOM is spatio-temporally invariant, unlike the equivalent achromatic masking, which is highest at high temporal and low spatial frequencies of the stimulus. Finally, chromatic XOM is independent of the orientation of the mask, unlike achromatic masking, which displays orientation dependent effects that historically have led to the modeling of orientationally selective luminance mechanisms in human vision.

Chromatic XOM is greater than achromatic and shows spatio-temporal invariance

We have found that chromatic XOM is significantly greater than achromatic XOM over the spatial and temporal frequency range at which masking could be measured (0.375 cpd–0.75 cpd; 2–4 Hz). For both subjects for each spatio-temporal configuration, the estimated slopes for masking were higher at isoluminance and the averaged chromatic to achromatic masking ratio significantly higher than unity. At temporal frequencies above 4 Hz, the rapid loss of contrast sensitivity of color vision means that there is insufficient stimulus contrast to

produce masking, which requires a mask contrast greater than 4–5 times threshold. Our results show little or no dependency of chromatic XOM on the spatio-temporal configurations used, and the data cluster into a single scale at medium-high mask contrasts (Figures 2–5). Our achromatic data, on the other hand, support the presence of XOM as shown previously (Baker & Meese, 2007; Baker, Meese, & Summers, 2007; Cass & Alais, 2006; Chen & Foley, 2004; Foley, 1994; Holmes & Meese, 2004; Meese & Baker, 2008; Meese, Holmes, et al., 2007; Meese, Summers, et al., 2007; Petrov et al., 2005; Ross & Speed, 1991) but show that achromatic TvC functions are spatio-temporally dependent, confirming previous results showing masking increasing in proportion to stimulus speed with strong masking occurring at high temporal and low spatial frequencies and weaker masking for low temporal and high spatial frequency conditions (Cass & Alais, 2006; Meese & Baker, 2008; Meese & Hess, 2004; Meese & Holmes, 2007; Meier & Carandini, 2002). Physiologically, XOS obtained from achromatic stimuli is also reported to be stronger at high temporal frequencies in cat cortex (Allison, Smith, & Bonds, 2001; Li et al., 2005).

The spatio-temporal range that is best for obtaining achromatic masking coincides with the range over which, based on primate data, inputs from the subcortical M cells dominate the contrast sensitivity function (Merigan & Maunsell, 1990, 1993). Hence, psychophysical studies have argued that monocular, achromatic XOM modulated by fast gratings may reflect gain controls originating in the magnocellular pathway or its projections (Baker et al., 2007; Cass & Alais, 2006; Meese & Baker, 2008; Meese & Holmes, 2007; Meier & Carandini, 2002). In contrast the chromatic XOM that we measure for our red-green stimuli is based on P cell responses or their projections, as these form the only subcortical pathway that has significant L/M cone opponency (Derrington, Krauskopf, & Lennie, 1984; Lee, Pokorny, Smith, Martin, & Valberg, 1990; Merigan, 1989; Merigan, Katz, & Maunsell, 1991). Hence, our results demonstrate a strong involvement of the P cell pathway in XOM and argue against the idea that M cells are exclusively involved in the mechanism of XOM.

Of course our results do not exclude an M cell involvement in achromatic XOM and suggest some interesting and important difference between the origins of chromatic and achromatic XOM. M cells have a nonlinear response function and show an early saturation as a function of contrast, suggesting their involvement in contrast normalization. The contrast saturation of the neuronal response is a key physiological factor in XOM. Physiological studies have suggested that monocular XOS may arise from the contrast saturation in the lateral geniculate nucleus (LGN) in the cat (Bonin, Mante, & Carandini, 2005; Carandini et al., 2002; Freeman et al., 2002; Li, Thompson, Duong, Peterson, & Freeman, 2006; Priebe & Ferster, 2006) and in primate originating from

non-oriented M cells (Solomon, Lee, & Sun, 2006), reflecting a revision of the view that XOM is of cortical origin. It has also been argued that the narrower response range of the early saturating primate M cells, in comparison to the more extended and linear P cell response function, generates a greater “need” for contrast normalization in the M cell pathway because normalization is required to extend the operating range of the neurons and prevent contrast saturation in the population as a whole, which would eliminate any capacity for population coding (Carandini & Heeger, 1994; Geisler & Albrecht, 1992; Heeger, 1992; Meese & Holmes, 2007).

As mentioned above, the P cell pathway has a more linear contrast response function than the M cell pathway and does not saturate within the contrast range of M cells (Kaplan & Shapley, 1982; Lennie & Movshon, 2005; Solomon & Lennie, 2005) and so it is interesting that despite this linearity we have found extensive XOM for chromatic stimuli, which are mediated by the P cell pathway. A rash conclusion based on our results would be that the linearity of subcortical neurons is not directly involved in the phenomenon of XOM since it occurs both for achromatic stimuli in the M cell spatio-temporal range, which has early saturation, and for P cells, which show little saturation. A more likely conclusion, however, is that chromatic and achromatic XOM have different physiological origins. This is supported by physiological data in primates showing normalization in M cells but not in the P cells of the LGN, but normalization in all cells at the cortical level of V1 (Solomon & Lennie, 2005; Solomon et al., 2006). This suggests that chromatic XOM, or chromatic contrast normalization, arises at a predominantly cortical site, a point to which we return later in the Discussion.

Chromatic XOM is isotropic and contrast invariant

A further difference that we have shown between chromatic and achromatic XOM is the lack of dependence on orientation for color vision and the contrast invariance of this isotropic effect. For achromatic vision, XOM is known to be orientation dependent (Petrov et al., 2005; Phillips & Wilson, 1984), and this effect was originally used as a basis for the modeling of orientationally selective, independent channels in luminance vision (Phillips & Wilson, 1984). Under the independent channel model, the lack of orientation dependence in masking in color vision would be interpreted to demonstrate the presence of detectors with very broad orientation tuning in color vision (Vimal, 1997). This interpretation, however, is not generally supported by psychophysical studies, which indicate quite similar orientation tuning (Beaudot & Mullen, 2005) and orientation discrimination (Webster et al., 1990) for chromatic and achromatic channels.

More recent approaches, however, consider XOM arising from overlaid stimuli to reflect nonlinear “cross channel” interactions, with the mask providing broadly tuned, modulatory (divisive) effects on the response to the test stimulus via the operation of contrast-gain control mechanisms (Bex, Mareschal, & Dakin, 2007; Carandini et al., 1997; Ding & Sperling, 2006; Foley, 1994; Geisler & Albrecht, 1992; Meese & Holmes, 2007; Ross & Speed, 1991; Solomon & Lennie, 2005). Thus, a more parsimonious interpretation of our results is that chromatic overlay masking reflects “cross-channel” gain control mechanisms that are isotropic, in comparison to the achromatic suppressive mechanisms that are known to be more orientationally selective (Phillips & Wilson, 1984). These differences in orientation tuning again point to underlying physiological differences between the mechanisms for chromatic and achromatic XOM.

The isotropic property and contrast invariance that we find for chromatic XOM is in keeping with physiological mechanisms of contrast normalization, which require broad tuning in the relevant stimulus dimension in order to maintain stimulus selectivity at all contrast levels. Our psychophysical results, if present at the physiological level, suggest that the orientation selectivity of chromatic cortical neurons (whether broad or narrow) will remain constant across different contrast levels.

Origins of the chromatic and achromatic differences in XOM

It seems likely that the significant differences we find in the magnitude, spatio-temporal invariance, and orientation selectivity of XOM between chromatic and achromatic contrast reflect differences in their physiological origins. Overlay masking, at least for achromatic stimuli, is thought to occur earlier in the visual pathway than surround masking because of its broad spatial and orientation tuning and because it includes activity at a monocular site (Baker & Meese, 2007; Baker et al., 2007; Cass & Alais, 2006; Petrov et al., 2005). Recently, however, it has been proposed that there are two sites at which XOM may occur, a subcortical monocular site as described above and a dichoptic site (Baker et al., 2007; Meese & Baker, 2008). Under dichoptic conditions, the properties of XOM change in comparison to the monocular condition; masking is significantly stronger, it is spatio-temporally invariant, and fails to be affected by adaptation (Baker et al., 2007; Meese & Baker, 2008), suggesting that these are the characteristics of cortical XOM. Moreover, there is physiological evidence in the cat for a monocular, subcortical site of XOM that fails to adapt and a binocular cortical site that shows adaptation (Li et al., 2005; Sengpiel & Vorobyov, 2005). Our results reported here for binocular chromatic XOM show a strong similarity to the dichoptic, achromatic XOM in terms of the properties of spatio-temporal invariance and the high

level of masking found. This lends support to the argument that chromatic masking is cortical in origin, which is also compatible with the linear responses of the subcortical P cells. We do not yet know whether chromatic XOM occurs dichoptically, which would provide additional support for a cortical origin.

Achromatic cortical cross-orientation suppression is thought to arise from untuned intracortical inhibition that forms a divisive normalization pool from many other cortical neurons tuned to different preferred orientations (Bonds, 1989; Carandini & Heeger, 1994; Carandini et al., 1997; DeAngelis et al., 1992; Heeger, 1992; Sengpiel & Vorobyov, 2005; Walker et al., 1998). All chromatic neurons in primate cortex demonstrate mechanisms of gain control, although the subcortical P cells do not (Solomon & Lennie, 2005; Solomon et al., 2006), supporting the existence of a cortical divisive normalization pool in color vision. Whether the psychophysical chromatic XOM reflects the responses of the non-oriented color selective neurons in the primate cortex, which show contrast invariant tuning for color, or the orientationally tuned neurons that respond to both chromatic and achromatic contrast is an issue that remains to be addressed in further experiments.

Acknowledgments

We thank Drs. Tim Meese and David Tolhurst for early discussion of the issue. This research was supported by a Canadian Institutes of Health Research (CIHR) grant MOP-10819 to K.T.M.

Commercial relationships: none.

Corresponding author: Kathy T. Mullen.

Email: kathy.mullen@mcgill.ca.

Address: McGill Vision Research, Department of Ophthalmology H4.14, 687 Pine Ave West, Montreal, Quebec, Canada H3A 1A1.

References

- Allison, J. D., Smith, K. R., & Bonds, A. B. (2001). Temporal-frequency tuning of cross-orientation suppression in the cat striate cortex. *Visual Neuroscience*, *18*, 941–948. [PubMed]
- Baker, D. H., & Meese, T. S. (2007). Binocular contrast interactions: Dichoptic masking is not a single process. *Vision Research*, *47*, 3096–3107. [PubMed]
- Baker, D. H., Meese, T. S., & Summers, R. J. (2007). Psychophysical evidence for two routes to suppression before binocular summation of signals in human vision. *Neuroscience*, *146*, 435–448. [PubMed]

- Beaudot, W. H., & Mullen, K. T. (2005). Orientation selectivity in luminance and color vision assessed using 2-d band-pass filtered spatial noise. *Vision Research*, *45*, 687–696. [PubMed]
- Bex, P. J., Mareschal, I., & Dakin, S. C. (2007). Contrast gain control in natural scenes. *Journal of Vision*, *7*(11):12, 1–12, <http://journalofvision.org/7/11/12/>, doi:10.1167/7.11.12. [PubMed] [Article]
- Blakemore, C., & Campbell, F. W. (1969). On the existence of neurones in the human visual system selectively sensitive to the orientation and size of retinal images. *The Journal of Physiology*, *203*, 237–260. [PubMed] [Article]
- Bonds, A. B. (1989). Role of inhibition in the specification of orientation selectivity of cells in the cat striate cortex. *Visual Neuroscience*, *2*, 41–55. [PubMed]
- Bonin, V., Mante, V., & Carandini, M. (2005). The suppressive field of neurons in lateral geniculate nucleus. *Journal of Neuroscience*, *25*, 10844–10856. [PubMed] [Article]
- Bradley, A., Switkes, E., & De Valois, K. (1988). Orientation and spatial frequency selectivity of adaptation to color and luminance gratings. *Vision Research*, *28*, 841–856. [PubMed]
- Bradley, A., Zang, L., & Thibos, L. N. (1992). Failures of isoluminance caused by ocular chromatic aberration. *Applied Optics*, *31*, 3657–3667.
- Breitmeyer, B. (1984). *Visual masking: An integrative approach* (pp. 270–286). New York: Oxford University Press.
- Breitmeyer, B. (2007). Visual masking: Past accomplishments, present status, future developments. *Advances in Cognitive Psychology*, *3*, 9–20.
- Campbell, F. W., & Kulikowski, J. J. (1966). Orientational selectivity of the human visual system. *The Journal of Physiology*, *187*, 437–445. [PubMed] [Article]
- Carandini, M., & Heeger, D. J. (1994). Summation and division by neurons in primate visual cortex. *Science*, *264*, 1333–1336. [PubMed]
- Carandini, M., Heeger, D. J., & Movshon, J. A. (1997). Linearity and normalization in simple cells of the macaque primary visual cortex. *Journal of Neuroscience*, *17*, 8621–8644. [PubMed] [Article]
- Carandini, M., Heeger, D. J., & Senn, W. (2002). A synaptic explanation of suppression in visual cortex. *Journal of Neuroscience*, *22*, 10053–10065. [PubMed] [Article]
- Cass, J., & Alais, D. (2006). Evidence for two interacting temporal channels in human visual processing. *Vision Research*, *46*, 2859–2868. [PubMed]
- Cavanagh, P., Tyler, C. W., & Favreau, O. E. (1984). Perceived velocity of moving chromatic gratings. *Journal of the Optical Society of America A, Optics and Image Science*, *1*, 893–899. [PubMed]
- Chen, C. C., & Foley, J. M. (2004). Pattern detection: Interactions between oriented and concentric patterns. *Vision Research*, *44*, 915–924. [PubMed]
- Cole, G. R., Hine, T., & McIlhagga, W. (1993). Detection mechanisms in L-, M-, and S-cone contrast space. *Journal of the Optical Society of America A, Optics and Image Science*, *10*, 38–51. [PubMed]
- DeAngelis, G. C., Robson, J. G., Ohzawa, I., & Freeman, R. D. (1992). Organization of suppression in receptive fields of neurons in cat visual cortex. *Journal of Neurophysiology*, *68*, 144–163. [PubMed]
- Derrington, A. M., Krauskopf, J., & Lennie, P. (1984). Chromatic mechanisms in lateral geniculate nucleus of macaque. *The Journal of Physiology*, *357*, 241–265. [PubMed] [Article]
- De Valois, R. L., & De Valois, K. K. (1988). *Spatial vision* (pp. 176–211, 263–290). New York: Oxford University Press.
- Ding, J., & Sperling, G. (2006). A gain-control theory of binocular combination. *Proceedings of the National Academy of Sciences of the United States of America*, *103*, 1141–1146. [PubMed] [Article]
- Eskew, R. T., McLellan, J. S., & Giulianini, F. (1999). Chromatic detection and discrimination. In K. R. Gegenfurtner & L. T. Sharpe (Eds.), *Color vision: From molecular genetics to perception* (pp. 345–368). Cambridge: Cambridge University Press.
- Foley, J. M. (1994). Human luminance pattern-vision mechanisms: Masking experiments require a new model. *Journal of the Optical Society of America A, Optics, Image Science, and Vision*, *11*, 1710–1719. [PubMed]
- Freeman, T. C., Durand, S., Kiper, D. C., & Carandini, M. (2002). Suppression without inhibition in visual cortex. *Neuron*, *35*, 759–771. [PubMed] [Article]
- Geisler, W. S., & Albrecht, D. G. (1992). Cortical neurons: Isolation of contrast gain control. *Vision Research*, *32*, 1409–1410. [PubMed]
- Graham, N. V. S. (1989). *Visual patterns analyzer* (pp. 181–193, 212–246). New York: Oxford University Press.
- Heeger, D. J. (1992). Normalization of cell responses in cat striate cortex. *Visual Neuroscience*, *9*, 181–197. [PubMed]
- Henning, G. B., & Wichmann, F. A. (2007). Some observations on the pedestal effect. *Journal of Vision*, *7*(1):3, 1–15, <http://journalofvision.org/7/1/3/>, doi:10.1167/7.1.3. [PubMed] [Article]

- Holmes, D. J., & Meese, T. S. (2004). Grating and plaid masks indicate linear summation in a contrast gain pool. *Journal of Vision*, 4(12):7, 1080–1089, <http://journalofvision.org/4/12/7/>, doi:10.1167/4.12.7. [PubMed] [Article]
- Howard, I. P. (1982). *Human visual orientation* (pp. 93–119). New York: John Wiley and Sons.
- Hubel, D. H., & Wiesel, T. N. (1959). Receptive fields of single neurones in the cat's striate cortex. *The Journal of Physiology*, 148, 574–591. [PubMed] [Article]
- Hubel, D. H., & Wiesel, T. N. (1963). Receptive fields of cells in striate cortex of very young, visually inexperienced kittens. *Journal of Neurophysiology*, 26, 994–1002. [PubMed]
- Hubel, D. H., & Wiesel, T. N. (1968). Receptive fields and functional architecture of monkey striate cortex. *The Journal of Physiology*, 195, 215–243. [PubMed] [Article]
- Hubel, D. H., Wiesel, T. N., & Stryker, M. P. (1977). Orientation columns in macaque monkey visual cortex demonstrated by the 2-deoxyglucose autoradiographic technique. *Nature*, 269, 328–330. [PubMed]
- Johnson, E. N., Hawken, M. J., & Shapley, R. (2008). The orientation selectivity of color-responsive neurons in macaque V1. *Journal of Neuroscience*, 28, 8096–8106. [PubMed] [Article]
- Kaplan, E., & Shapley, R. M. (1982). X and Y cells in the lateral geniculate nucleus of macaque monkeys. *The Journal of Physiology*, 330, 125–143. [PubMed] [Article]
- Lee, B. B., Pokorny, J., Smith, V. C., Martin, P. R., & Valberg, A. (1990). Luminance and chromatic modulation sensitivity of macaque ganglion cells and human observers. *Journal of the Optical Society of America A, Optics and Image Science*, 7, 2223–2236. [PubMed]
- Lennie, P., & Movshon, J. A. (2005). Coding of color and form in the geniculostriate visual pathway (invited review). *Journal of the Optical Society of America A, Optics, Image Science, and Vision*, 22, 2013–2033. [PubMed]
- Levitt, J. B., & Lund, J. S. (1997). Contrast dependence of contextual effects in primate visual cortex. *Nature*, 387, 73–76. [PubMed]
- Li, B., Peterson, M. R., Thompson, J. K., Duong, T., & Freeman, R. D. (2005). Cross-orientation suppression: Monoptic and dichoptic mechanisms are different. *Journal of Neurophysiology*, 94, 1645–1650. [PubMed] [Article]
- Li, B., Thompson, J. K., Duong, T., Peterson, M. R., & Freeman, R. D. (2006). Origins of cross-orientation suppression in the visual cortex. *Journal of Neurophysiology*, 96, 1755–1764. [PubMed] [Article]
- Meese, T. S., & Baker, D. H. (2008). Spatiotemporal properties of cross-orientation masking: Speed computation precedes ipsiocular suppression, and interocular suppression is scale invariant. *Journal of Vision*.
- Meese, T. S., Challinor, K. L., & Summers, R. J. (2008). A common contrast pooling rule for suppression within and between the eyes. *Visual Neuroscience*, 25, 585–601. [PubMed]
- Meese, T. S., & Hess, R. F. (2004). Low spatial frequencies are suppressively masked across spatial scale, orientation, field position, and eye of origin. *Journal of Vision*, 4(10):2, 843–859, <http://journalofvision.org/4/10/2/>, doi:10.1167/4.10.2. [PubMed] [Article]
- Meese, T. S., & Holmes, D. J. (2007). Spatial and temporal dependencies of cross-orientation suppression in human vision. *Proceedings of the Royal Society B: Biological Sciences*, 274, 127–136. [PubMed] [Article]
- Meese, T. S., Holmes, D. J., & Challinor, K. L. (2007). Remote facilitation in the Fourier domain. *Vision Research*, 47, 1112–1119. [PubMed]
- Meese, T. S., Summers, R. J., Holmes, D. J., & Wallis, S. A. (2007). Contextual modulation involves suppression and facilitation from the center and the surround. *Journal of Vision*, 7(4):7, 1–21, <http://journalofvision.org/7/4/7/>, doi:10.1167/7.4.7. [PubMed] [Article]
- Meier, L., & Carandini, M. (2002). Masking by fast gratings. *Journal of Vision*, 2(4):2, 293–301, <http://journalofvision.org/2/4/2/>, doi:10.1167/2.4.2. [PubMed] [Article]
- Merigan, W. H. (1989). Chromatic and achromatic vision of macaques: Role of the P pathway. *Journal of Neuroscience*, 9, 776–783. [PubMed] [Article]
- Merigan, W. H., Katz, L. M., & Maunsell, J. H. (1991). The effects of parvocellular lateral geniculate lesions on the acuity and contrast sensitivity of macaque monkeys. *Journal of Neuroscience*, 11, 994–1001. [PubMed] [Article]
- Merigan, W. H., & Maunsell, J. H. (1990). Macaque vision after magnocellular lateral geniculate lesions. *Visual Neuroscience*, 5, 347–352. [PubMed]
- Merigan, W. H., & Maunsell, J. H. (1993). How parallel are the primate visual pathways? *Annual Review of Neuroscience*, 16, 369–402. [PubMed]
- Morrone, M. C., Burr, D. C., & Maffei, L. (1982). Functional implications of cross-orientation inhibition of cortical visual cells. I. Neurophysiological evidence. *Proceedings of the Royal Society of London B: Biological Sciences*, 216, 335–354. [PubMed]
- Peirce, J. W. (2007). The potential importance of saturating and supersaturating contrast response functions in visual cortex. *Journal of Vision*, 7(6):13, 1–10, <http://>

- journalofvision.org/7/6/13/, doi:10.1167/7.6.13. [PubMed] [Article]
- Pelli, D. G. (1985). Uncertainty explains many aspects of visual contrast detection and discrimination. *Journal of the Optical Society of America A, Optics and Image Science*, 2, 1508–1532. [PubMed]
- Petrov, Y., Carandini, M., & McKee, S. (2005). Two distinct mechanisms of suppression in human vision. *Journal of Neuroscience*, 25, 8704–8707. [PubMed] [Article]
- Phillips, G. C., & Wilson, H. R. (1984). Orientation bandwidths of spatial mechanisms measured by masking. *Journal of the Optical Society of America A, Optics and Image Science*, 1, 226–232. [PubMed]
- Priebe, N. J., & Ferster, D. (2006). Mechanisms underlying cross-orientation suppression in cat visual cortex. *Nature Neuroscience*, 9, 552–561. [PubMed]
- Ross, J., & Speed, H. D. (1991). Contrast adaptation and contrast masking in human vision. *Proceedings of the Royal Society B: Biological Sciences*, 246, 61–69. [PubMed]
- Ross, J., Speed, H. D., & Morgan, M. J. (1993). The effects of adaptation and masking on incremental thresholds for contrast. *Vision Research*, 33, 2051–2056. [PubMed]
- Sankeralli, M. J., & Mullen, K. T. (1996). Estimation of the L-, M- and S-cone weights of the post-receptoral detection mechanisms. *Journal of the Optical Society of America A*, 13, 906–915.
- Sengpiel, F., & Vorobyov, V. (2005). Intracortical origins of interocular suppression in the visual cortex. *Journal of Neuroscience*, 25, 6394–6400. [PubMed] [Article]
- Sharon, D., & Grinvald, A. (2002). Dynamics and constancy in cortical spatiotemporal patterns of orientation processing. *Science*, 295, 512–515. [PubMed]
- Smith, V. C., & Pokorny, J. (1975). Spectral sensitivity of the foveal cone photopigments between 400 and 500 nm. *Vision Research*, 15, 161–171. [PubMed]
- Snowden, R. J. (1992). Orientation bandwidth: The effect of spatial and temporal frequency. *Vision Research*, 32, 1965–1974. [PubMed]
- Snowden, R. J., & Hammett, S. T. (1998). The effects of surround contrast on contrast thresholds, perceived contrast and contrast discrimination. *Vision Research*, 38, 1935–1945. [PubMed]
- Solomon, J. A., Sperling, G., & Chubb, C. (1993). The lateral inhibition of perceived contrast is indifferent to on-center/off-center segregation, but specific to orientation. *Vision Research*, 33, 2671–2683. [PubMed]
- Solomon, S. G., Lee, B. B., & Sun, H. (2006). Suppressive surrounds and contrast gain in magnocellular-pathway retinal ganglion cells of macaque. *Journal of Neuroscience*, 26, 8715–8726. [PubMed] [Article]
- Solomon, S. G., & Lennie, P. (2005). Chromatic gain controls in visual cortical neurons. *Journal of Neuroscience*, 25, 4779–4792. [PubMed] [Article]
- Tolhurst, D. J., & Heeger, D. J. (1997). Comparison of contrast-normalization and threshold models of the responses of simple cells in cat striate cortex. *Visual Neuroscience*, 14, 293–309. [PubMed]
- Truchard, A. M., Ohzawa, I., & Freeman, R. D. (2000). Contrast gain control in the visual cortex: Monocular versus binocular mechanisms. *Journal of Neuroscience*, 20, 3017–3032. [PubMed] [Article]
- Vimal, R. L. (1997). Orientation tuning of the spatial-frequency-tuned mechanisms of the red-green channel. *Journal of the Optical Society of America A*, 14, 2622–2632.
- Vimal, R. L. (1998). Spatial-frequency tuning of sustained nonoriented units of the red-green channel. *Journal of the Optical Society of America A, Optics, Image Science, and Vision*, 15, 1–15. [PubMed]
- Vimal, R. L. (2002). Spatial-frequency-tuned mechanisms of the red-green channel estimated by oblique masking. *Journal of the Optical Society of America A, Optics, Image Science, and Vision*, 19, 276–288.
- Walker, G. A., Ohzawa, I., & Freeman, R. D. (1998). Binocular cross-orientation suppression in the cat's striate cortex. *Journal of Neurophysiology*, 79, 227–239. [PubMed] [Article]
- Webster, M. A., De Valois, K. K., & Switkes, E. (1990). Orientation and spatial-frequency discrimination for luminance and chromatic gratings. *Journal of the Optical Society of America A, Optics and Image Science*, 7, 1034–1049. [PubMed]
- Xing, J., & Heeger, D. J. (2000). Center-surround interactions in foveal and peripheral vision. *Vision Research*, 40, 3065–3072. [PubMed]
- Yu, C., & Levi, D. M. (2000). Surround modulation in human vision unmasked by masking experiments. *Nature Neuroscience*, 3, 724–728. [PubMed]